PCCP

ROYAL SOCIETY OF CHEMISTRY

PAPER

View Article Online
View Journal | View Issue

Cite this: *Phys. Chem. Chem. Phys.*, 2026, **28**, 3227

Heterogeneous translational dynamics of succinonitrile in the plastic crystalline phase

Keiko Nishikawa *[a] and Kozo Fujii[b]

Received 14th August 2025,
Accepted 12th January 2026

DOI: 10.1039/d5cp03114a

rsc.li/pccp

A plastic crystal (PC) has a crystalline phase characterized by disordered molecular orientations while maintaining a regular lattice of molecular positions. Recent studies have reported heterogeneous dynamics within the PC phase of several ionic PCs (IPCs). This study investigates whether similar dynamics exist in a molecular PC (MPC) by examining the temperature dependence of the spin–lattice relaxation time (T_1) and the spin–spin relaxation time (T_2) of succinonitrile (NC–CH_2–CH_2–CN) using pulsed low-frequency nuclear magnetic resonance. The results reveal a splitting of T_2 values, which are sensitive to translational motion, within the PC phase, indicating the presence of heterogeneous translational dynamics in both MPCs and IPCs. These findings suggest that such heterogeneous dynamics are an intrinsic, yet previously overlooked, property common to plastic crystals regardless of their ionic or molecular nature.

1. Introduction

A plastic crystal (PC) has a crystalline phase in which the orientations of the constituent molecules are disordered, while their centers of mass remain arranged in a regular crystalline lattice. PCs are typically formed by quasi-spherical molecules that undergo vigorous rotational motion or exhibit significant orientational disorder.[1] As temperature increases, these materials usually undergo a phase sequence: from a regular crystalline phase at low temperatures, through the PC phase, and finally into the liquid phase. Initially, physical chemists and condensed matter physicists investigated molecular PCs (MPCs)—PCs composed of molecular units—as an intermediate state between the liquid and the normal crystalline phases. As a result, extensive fundamental research has been devoted to MPCs, particularly focusing on their thermodynamic properties and structural characteristics.[1–6]

A number of compounds related to ionic liquids (ILs) that exhibit PC phases have been discovered in recent years.[7–10] These compounds are ionic rather than molecular and are known as ionic PCs (IPCs) or organic IPCs (OIPCs). Since the publication of the seminal work by MacFarlane *et al.*[7] IPCs have attracted increasing attention due to their diverse functionalities, particularly their potential applications as solid-state electrolytes.[7–14] These materials are ionic conductors, and one of the key factors governing their ionic conductivity is the dynamic behavior of their constituent cations and anions. Given the relatively slow dynamics in IPCs and the corresponding time scales of these processes, nuclear magnetic resonance (NMR) spectroscopy is particularly well suited for investigating such dynamics.[15–17] Accordingly, numerous NMR studies on IPCs have revealed some novel phenomena—one of which is the coexistence of two distinct types of dynamics, or heterogeneous dynamics, in the PC phase. To the best of our knowledge, the first report of heterogeneous dynamics in IPCs was published by Ikeda and Ishida,[18–21] who primarily investigated ammonium salts and observed two distinct NMR spin–lattice relaxation times (T_1) and two distinct spin–spin relaxation times (T_2) for each sample. Following the work of the Australian group led by Forsyth and MacFarlane, who demonstrated the potential of IPCs as solid electrolytes,[7] systematic and coordinated NMR investigations of IPCs were undertaken.[17,22–28] In this context, several studies focused on heterogeneous dynamics as revealed by NMR, using methods such as spectral linewidth analysis[22–25] and imaging.[26–28]

For many years, we have investigated the relationship between the phase transitions of ILs and the dynamics of their constituent ions using NMR relaxation time measurements (T_1 and T_2).[29–39] Measurements on *N*-butyl-*N*-methylpiperidinium hexafluorophosphate ($[C_4mpip]PF_6$)[37] and *N*,*N*-diethylpyrrolidinium bis(fluorosulfonyl)amide ($[C_2epyr][FSA]$)[38,39]—both of which exhibit PC phases—revealed the presence of two distinct T_2 values within a certain temperature range in the PC phase. We interpreted the splitting of the T_2 values as indicating the emergence of heterogeneous translational dynamics. We believed that this heterogeneity in the dynamics stems from differences in the translational motion of ions

[a] *Department of Chemistry, Graduate School of Science, Chiba University, Chiba-shi, Chiba 263-8522, Japan. E-mail: k.nishikawa@faculty.chiba-u.jp*
[b] *Center for Analytical Instrumentation, Chiba University, Chiba-shi, Chiba 263-8522, Japan*

present in two distinct regions: namely, the core region of the IPC crystallite (the low-mobility component) and the surrounding surface region/grain boundary (the high-mobility component).[38,39]

The novel phenomenon of heterogeneous dynamics in the PC phase has so far been observed only in IPCs.[18–28,37–39] This raises the question of whether the same phenomenon also occurs in MPCs. The present study aims to clarify whether this behavior arises from ionic *versus* molecular differences, or whether it is an intrinsic characteristic of the PC state.

For this purpose, succinonitrile (SN, (NC–CH_2–CH_2–CN)) was selected as the sample because it is a well-known representative MPC.[6] Moreover, the regular crystalline, PC, and liquid phases of SN all occur within a temperature range accessible to our instrumentation. If heterogeneous components are present in the PC phase, measurements must be performed across the normal crystalline, PC, and liquid phases to determine how these components are related. In addition, fascinate Li-ion conductivity behavior has been reported in systems where SN is doped with Li salts, making it a promising candidate for solid-state electrolytes.[40] In this context, the present study provides a foundation for understanding the intrinsic physical properties of SN, which can inform such applied research.

Numerous NMR studies have been conducted to investigate the dynamics of ILs and related IPCs,[15–39] and high-frequency NMR (HF-NMR) is a commonly employed technique in such investigations.[15–17,22–26] However, our approach differs from conventional methods in two key respects:

(1) we use pulsed low-frequency NMR (LF-NMR) spectroscopy, and

(2) we observe T_1 and T_2 in combination.

A few additional details on item (1) are presented here. While HF-NMR is limited to liquids and solutions, LF-NMR can be applied to liquids, viscous fluids, glasses, PCs, and regular crystals —an essential capability for investigating dynamic behavior across different phases. In HF-NMR, signals from nuclides in distinct environments can be resolved separately, and in some cases the corresponding correlation time τ_c can also be estimated. In contrast, LF-NMR produces overlapping signals from nuclides in different environments, which cannot be separated. Nevertheless, LF-NMR relaxation time measurements yield coarse-grained information on molecular or ionic–molecular motion dynamics across all phases,[29–32,35–39] thereby offering a broader perspective on the phenomena and complementing methods that provide more detailed insights. Regarding item (2), T_1 and T_2 are primarily sensitive to reorientational and translational motions, respectively.[15,16,39,41] Measuring the temperature dependence of T_1 and T_2 together makes it possible to detect phase changes in the sample and to determine whether these changes are driven by reorientational or translational dynamics.[29–32,35–39]

2. Experimental

SN was purchased from Tokyo Kasei Co., Ltd, with a stated purity greater than 99%. The sample was used without further purification. At room temperature, SN is waxy, making direct placement into an NMR tube difficult. To facilitate loading, SN was dissolved in dichloromethane, and the resulting solution was transferred into the NMR tube. Dichloromethane was first evaporated in air. After visually confirming that it had been sufficiently removed, the sample was vacuum-dried at approximately 10^{-2} Pa and room temperature for 30 min. The tube was then flame-sealed promptly to prevent moisture contamination.

A pulse NMR spectrometer with a ^{1}H resonance frequency of 25 MHz (MV25, Japan REDOX) was used to measure ^{1}H relaxation times. Owing to the low resonance frequency, chemical shift dispersion was minimal, enabling observation of the overall dynamics of the ^{1}H nuclei in SN rather than site-specific motions. T_1 values were obtained using the inversion–recovery method,[41] while T_2 values were measured using the Carr–Purcell–Meiboom–Gill method for the liquid phase and the solid–echo method for the crystalline and PC phases.[41]

The measurements were carried out over the temperature range of 220–360 K, typically in 10-K increments, and in 5-K increments near the phase transition region. The temperature dependences of the relaxation times associated with the phase change of this sample exhibited a pronounced thermal history; therefore, the experimental setup was carefully controlled. The details for standardizing are described in Sections 3.2 and 3.3.

3. Results and discussion

3.1. Background information

Fig. 1 shows the chemical structure of SN, with only the *gauche* configuration presented.

Before addressing the main topic—the temperature dependence of the NMR relaxation times (T_1 and T_2)—the phase behavior of SN is outlined based on differential scanning calorimetry (DSC) results.[42] The melting point of SN is 330 K. At room temperature, it is a waxy solid that undergoes a phase transition to another crystalline form at approximately 233 K. In this work, the waxy phase is referred to as Phase I, and the low-temperature crystalline phase as Phase II. The transition temperature from Phase II to Phase I is 233 K.

The structures of the respective phases of SN reported to date are summarized here. For Phase II, structural analysis by powder X-ray diffraction has shown this phase to be a conventional regular crystalline phase with the $P2_1/a$ space group and

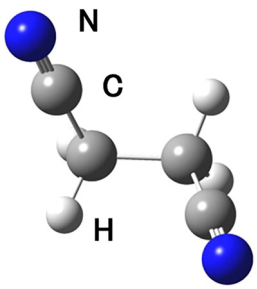

Fig. 1 Succinonitrile in the *gauche* conformation.

a gauche-type molecular arrangement.[43] Phase I is a PC phase with a body-centered cubic (bcc) structure.[43,44] In this phase, the molecules occupy special lattice points and therefore must exhibit statistical $m\bar{3}m$ symmetry. To satisfy this requirement,[45,46] the molecules must either (1) rotate freely so that they can be considered statistically spherical, or (2) have the CH_2–CH_2 axis evenly distributed along the four diagonal directions of the cubic lattice, with the CN groups statistically evenly distributed or freely rotating around the CH_2–CH_2 axis. Based on previous reports,[6,43–47] the PC phase structure of SN corresponds to case (2). In many substances with a PC phase, free rotation of the entire molecule or ion often results in complete directional uniformity. In contrast, in SN, the PC phase is formed through a combination of partial directional disorder along a specific molecular axis and partial or free rotation of the molecules around that axis.

SN is one of the representative compounds associated with the long-standing topic of rotational isomerism in the XCH_2–CH_2X molecular system.[6,48,49] As mentioned earlier, the *gauche* structure is adopted in Phase II (regular crystalline phase).[43] In Phase I (PC phase), the main component is also *gauche* (approximately 80%), although its abundance ratio varies slightly with temperature.[47] The *gauche* form is the major component likewise in the liquid state.[47] The predominance of the *gauche* configuration in all phases is attributed to its polarity, which stabilizes the structure through electrostatic interactions between polar molecules.

Background information on the NMR relaxation times relevant for data analysis and interpretation is provided in our previous work.[38,39]

3.2. Temperature dependence of spin–lattice relaxation time (T_1)

When the dipole–dipole relaxation mechanism is predominant, the molecular reorientational and intramolecular rotational motions of viscous liquids and solids are generally reflected primarily in the T_1 values.[15,16,41] The rotational and conformational changes of SN are discussed below.

Fig. 2 shows the temperature dependence of T_1. The sample exhibits supercooling and superheating phenomena near the phase transitions, which may contribute to the observed thermal history effects. To standardize the initial conditions, several experimental sets were repeated with starting temperatures of 200 K (Phase II) for the heating process and 370 K (liquid state) for the cooling process. Measurements at each temperature were taken at least 10 min after reaching the set temperature. In the figure, T_1 data for the heating process are plotted as closed black circles. Because superheating is generally less likely to occur than supercooling, the values obtained during heating were adopted as the T_1 values at each temperature. In the vicinity of the phase transition, where superheating and/or supercooling occurred, T_1 values for the heating and cooling processes differed. In this temperature range, results from the cooling process are shown as open squares. This difference in T_1 is attributed to structural relaxation phenomena, such as superheating and supercooling.[29–32,35–37,39] In other words, it serves as a useful indicator of whether a phase transition is taking place. The two broken lines in Fig. 2 mark the phase transition temperatures determined by the DSC experiment.[42] Each error bar for the experimental T_1 values is smaller than the corresponding symbol size.

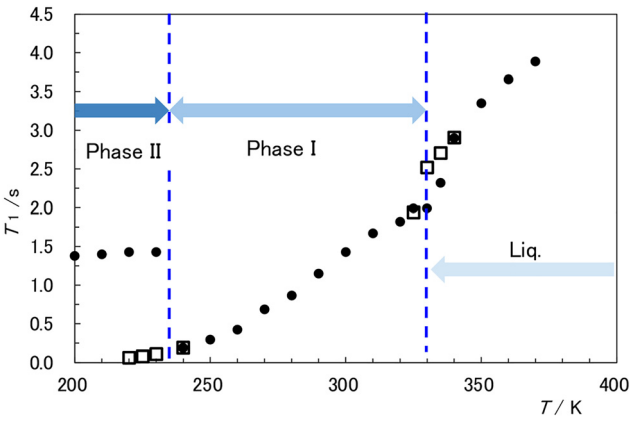

Fig. 2 Temperature dependence of ^{1}H-T_1 values. Closed circles and open squares represent values obtained during the heating and cooling processes, respectively. The two broken lines indicate phase transition temperatures determined by the DSC experiment.[42]

We first discuss the overall temperature dependence of T_1, with reference to the temperature-dependent behaviour of glycerol T_1 (and T_2) as a typical viscous sample described in the Supplementary Information of our previous paper.[29,37] For SN, a discontinuous change in the T_1 plot is observed around 230 K–240 K, corresponding to the transition from Phases II to Phase I observed in the DSC data at 233 K.[42] As indicated by the open square symbols in Fig. 2, the sample is prone to supercooling phenomena in the phase transition here. The different behaviour in the two phases reflects the different rotational and intramolecular dynamics of the SN molecule in each phase. As mentioned above, Phase II is a regular crystal phase, whereas Phase I is a PC phase in which molecules undergo free or partial rotation.[1–6] The jump in T_1 values at approximately 230–240 K is thus associated with the onset of overall free or partial molecular rotation with large amplitude. Diffraction experiments[43–46] indicate that this motion corresponds to a partial, uniaxial rotation around the CH_2–CH_2 axis.

As indicated by the DSC results, the transition from Phase I to the liquid phase occurred at 330 K.[42] Though the T_1 values varied relatively smoothly with temperature in this temperature region, a slight yet distinct difference was observed between the heating and cooling processes. This finding suggests that the magnetic dipole–dipole interactions associated with the reorientational motions of SN molecules in Phase I and in the liquid phase are similar in magnitude but not identical. In other words, the change in magnetic dipole interactions that occurs during the phase transition takes place over a large distance rather than a short one, as would be expected from the T_1 relaxation equations.[39,41] From the perspective of rotational dynamics, this transition can be attributed to a change from uniaxial rotation about the CH_2–CH_2 axis in Phase I to complete, unrestricted molecular rotation in the liquid phase.

Experiments using [C_2epyr][FSA] as a sample have confirmed that in the PC phase, where the ions rotate freely, the T_1 values of the PC and liquid phases are smoothly connected without

discontinuity.[39] Previous diffraction experiments[43–46] and computer simulation studies[47] have already established that SN molecules in the PC phase undergo uniaxial rotation. The present findings indicate that the difference between free and restricted axial rotations, in terms of molecular reorientation dynamics, was also clearly reflected in the T_1 measurements.

Dielectric relaxation measurements provide information on molecular motion in the PC phase.[49–51] This experimental technique is particularly effective for studying the details of molecular rotational motion, providing more information than our low-frequency NMR-T_1 measurements (which are sensitive to molecular rotational motion) in this study. However, NMR-T_2 measurements provide information about the translational motion of molecules that cannot be obtained *via* dielectric measurements. Therefore, dielectric relaxation methods and relaxation time measurements from NMR are complementary. Below, we discuss the translational motion obtained from NMR-T_2.

3.3. Temperature dependence of spin–spin relaxation times (T_2)

As previously noted, the dipole–dipole relaxation mechanism is generally dominant in viscous liquids and glassy samples.[41] In this mechanism, the translational or diffusive motions of molecules are the primary contributors to T_2,[41] with experimental evidence presented in our previous study.[39]

Fig. 3 shows the temperature dependence of the ^{1}H-T_2 values. As with T_1, the T_2 data from the heating process---where the likelihood of non-equilibrium phase changes is low—were adopted for the entire measurement range and are shown as closed circles. The cooling-process data are indicated by open squares only when necessary, such as when the T_2 values differed between heating and cooling. As described in Section 3.2 for the T_1 results, such differences serve as a useful indicator for identifying phase transitions.[29–32,35–37,39] Similar to [C_2epyr][FSA],[39] the T_2 values of ScN split into two components beginning in the intermediate temperature region of the

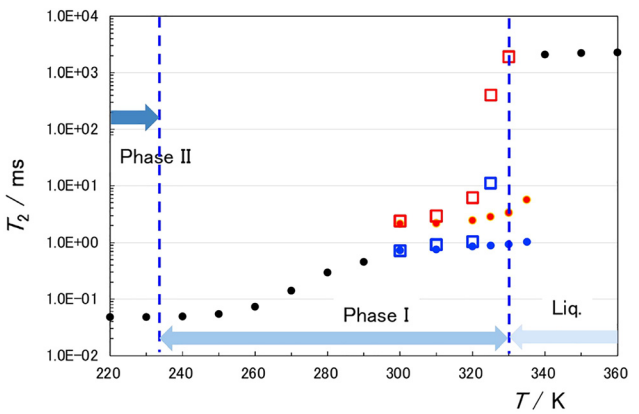

Fig. 3 Temperature dependence of ^{1}H-T_2 values obtained during the heating process (closed circles) and the cooling process (open squares). Black symbols show T_2 values analysed using the single-component assumption, whereas blue and red symbols correspond to the hard and soft components obtained from the two-component assumption.

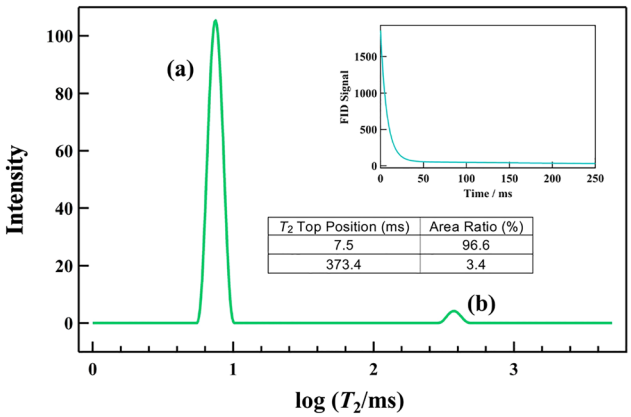

Fig. 4 The T_2 distribution for 325 K data during the cooling process. The inset shows the original FID signal. In the distribution graph, the peak at 7.5 ms (a) represents the hard component with an abundance ratio of 0.966, while the peak at 373.4 ms (b) represents the soft component with an abundance ratio of 0.034.

PC phase. Examples of FID curves and their fitting analyses are provided in the SI. To demonstrate this phenomenon more clearly, the T_2 distribution for the 325 K data in cooling process is shown in Fig. 4. This distribution was calculated from the corresponding FID data illustrated in the upper right of Fig. 4. As is evident from the figure, the T_2 values are clearly divided into two distinct groups. The T_2 values analyzed under the one-component assumption are shown as black symbols in Fig. 3 and are denoted as T_2 one-component (T_2^{1C}). Above 300 K, the two-component assumption provided a better fit for the data. The resulting T_2 values are referred to as T_2^{hard} (closed blue circles in Fig. 3) and T_2^{soft} (closed red circles in Fig. 3).

The open squares represent the values obtained during the cooling process, with the same color coding as in the heating process. Superheating and supercooling phenomena were observed near 330 K, corresponding to the melting temperature determined by the DSC experiment.[42]

This sample is prone to superheating during the heating process and supercooling during the cooling process. We shall verify this phenomenon at the melting and crystallization temperature. Regarding the data points indicated by the closed red and blue circles at 335 K in Fig. 3 (heating process), it may appear at first glance that heterogeneous dynamics discussed in Section 3.4 exist even in the liquid phase. However, this is due to the sample exhibiting superheating. That is, during heating, it indicates that the sample persists as a plastic crystal even after exceeding the melting point due to superheating. When the sample is heated to 340 K (closed black circle), it exhibits different T_2 values compared to those during heating process and indicates a homogeneous motion state. During the cooling process, as shown by the open squares in Fig. 3, supercooling is observed even below the melting point.

The measurements were systematically repeated multiple times. In the temperature range of 300–320 K, the T_2 values varied considerably between experiments. This indicated that the temperature dependence of the physical properties

associated with the sample's phase change was strongly influenced by thermal history. Consequently, the experimental configuration was carefully optimized, including standardization of the initial conditions and the use of adequate waiting times after reaching each measurement temperature. These procedures reduced the fluctuations in T_2 values to a reasonably acceptable range. In the 300–320 K region, the errors in T_2^{soft} were approximately ±30%, making this the most challenging region for reliable value determination. In contrast, the errors for the other T_2 values were smaller than ±5%.

3.4. Heterogeneous dynamics observed in T_2

This section examines in detail the separation of the T_2 values, which is shown in Fig. 3 and 4. In the PC phase of this sample at temperatures above 300 K, the free induction decay (FID) curves exhibited both fast and slow decay components, as observed previously for $[C_4mpip]PF_6$[37] and $[C_2epyr][FSA]$.[38,39] This separation indicates the presence of two kinetic modes with distinct ^{1}H-T_2 values. The fast decay component in the FID curve corresponded to a smaller T_2 value, representing hard or less mobile motions, whereas the slow decay component corresponded to a larger T_2 value, representing soft or highly mobile motions. These are referred to as T_2^{hard} (blue symbols in Fig. 3) and T_2^{soft} (red symbols in Fig. 3), respectively. For comparison, the T_2 values obtained from a one-component analysis (black circles in Fig. 3) are denoted as T_2^{1C}. Because the T_2 measurements were performed using low-frequency pulsed NMR, the resulting data represent an overall superposition of the ^{1}H nuclei within the SN molecule, rather than signals from individual ^{1}H in distinct environments.[29–32,35–39] The T_2 values can be interpreted as reflecting the translational or diffusive motion of the entire SN molecule. In other words, two types of translational motion of SN molecules were present at temperatures above 300 K in the PC phase. Similar phenomena have been reported as heterogeneous dynamics of ionic molecules in several IPCs,[14,23–28] including $[C_4mpip]PF_6$[37] and $[C_2epyr][FSA]$.[38,39] The present results for SN indicate that such heterogeneous translational dynamics is not unique to IPCs but also occurs in MPCs. This suggests that the presence of heterogeneous translational dynamics may be a general feature of all PC phases, whether ionic or molecular.

Fig. 5 shows the presence ratios of the soft components. Only the values obtained during the heating process are denoted. The error bars reflect the large variations in the values, which can be attributed to the formation process of the region producing T_2^{soft}. Between 300 K and 330 K (melting temperature), the ratio increased only slightly with increasing temperature, remaining below 0.1. Even just before the melting point, the increase was not pronounced. This behavior contrasts with that of $[C_2epyr][FSA]$, where the ratio increased rapidly as the melting point was approached and eventually reached 1.0.[38,39]

3.5. Model explaining the heterogeneous dynamics

As stated in Section 3.1, structural analysis of the PC phase of SN was conducted using X-ray diffraction. This revealed that the

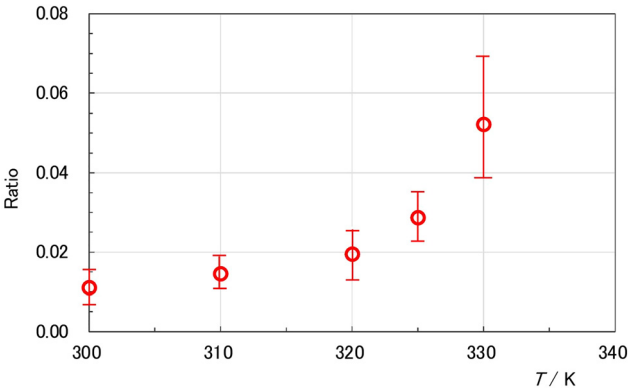

Fig. 5 Temperature dependence of the soft component ratio for ^{1}H-T_2.

diffraction pattern exhibits a bcc structure,[43] and it has been reported that this pattern is maintained up to the melting point even upon temperature increase.[52] That is to say, it has been confirmed that domains possessing a crystalline lattice exist within the PC phase. Based on the structural analysis results, we propose the following model to explain the emergence of heterogeneous dynamics in SN. This model is the same as that proposed by MacFarlane and Forsyth's group[23–28] and by us for $[C_2epyr][FSA]$.[38,39] In the PC phase, SN exists in a polycrystalline state. Each crystallite comprises a core region and surrounding surface region. When crystallites are in close proximity, these surface regions may also be described as grain boundaries. Hereafter, the surface regions and grain boundaries shall collectively be referred to as the surrounding regions. The translational motion of molecules in the core region corresponds to T_2^{hard}, whereas that in the surrounding regions correspond to T_2^{soft}. The core region forms the PC phase, where the centers of gravity of the molecules arrange in a regular lattice, but the molecular orientations are melted due to rotational motion or significant rotational disorder. By contrast, the surrounding regions exhibit structures that differ from that of the core, thereby mitigating the abrupt discontinuity at the interface. Whether the surrounding structures represent merely loosened forms of the core or are disordered to the extent of being amorphous remains unclear. From the perspective of translational dynamics of SN molecules, however, the core and surrounding regions can be treated as distinct regions, giving rise to the T_2^{hard} and T_2^{soft} components, respectively (see Fig. 3 and 4). The existence of the two kinds of regions, core and surrounding regions, were also clearly shown in the NMR-imaging for other IPCs by Romanenko *et al.*[28,29] Furthermore, a study of molecular dynamics simulations reported that a surface layer distinct from the core phase possessing a crystal lattice appears and grows with increasing temperature for the methyl(diethyl)-isobutylphosphonium hexafluorophosphate ($[P_{122i4}]PF_6$) belonging to the IPC.[53]

The ratio of the surrounding region, namely the proportion of the soft component, is highly susceptible to thermal history. This model provides an explanation for our consistent observations. The primary factor determining the ratio is the size of the crystallites. The size varies depending on the thermal history,

for example whether the sample was cooled rapidly or slowly during crystallization. Although experiments deliberately varying the cooling rate to set crystallization conditions were not conducted this time, performing such experiments may validate the model.

We discuss possibilities of two-state models distinct from the aforementioned model of core and surrounding regions. Examples include the existence of regions with different lattice defects or the presence of two types of PC regions. As the T_2 values indicated Fig. 3 and 4 clearly form two distinct groups which exhibite significantly difference in their motion activity ranging from several to tens of times, it is unlikely that these two groups are accounted for by distinct regions of lattice defects. Furthermore, regarding the state of the sample shown in Fig. 4, visual inspection reveals the presence of a jelly-like mass surrounded by wet region, indicating the existence of the two states: core and surrounding regions. Additionally, X-ray diffraction experiments demonstrate that the PC region exhibits a simple bcc structural pattern.[43] This makes the emergence of two crystalline states with significantly different structures unlikely.

We have explored alternative methods using NMR-T_2 measurements to detect this phenomenon, and we have conducted practical experiments. One approach is comparing densities using two distinct density measurement techniques. Specifically, these are a density measurement targeting only the portion forming the crystal lattice (deriving lattice constants from X-ray diffraction patterns) and a density measurement method encompassing both the core region and surrounding region (deriving density from X-ray absorption coefficients). Another approach is small-angle X-ray scattering experiments to detect mesoscale heterogeneous regions. These two types of experiments support the validity of the two-state model we proposed. We will report these results in the near future.

3.6. Phase transition

From here, the phenomenon is discussed in relation to phase transitions. The present experimental results show that the core and surrounding regions emerge abruptly at approximately 300 K. The key question to be resolved is which of the following scenarios applies:

(1) at temperatures below 300 K, a portion of the core region constituting the PC phase undergoes a phase transition to the surface region; or

(2) the surface regions are already present at lower temperatures, and a phase transition driven by translational motion occurs at around 300 K.

The proportion of the soft component yielding T_2^{soft} was small (approximately 1%), and the T_2^{hard} and T_2^{soft} values were close at around 300 K. Consequently, the present NMR relaxation measurements cannot definitively resolve the question posed above. Nevertheless, visual observation revealed that the sample in Phase II (ordered crystal) appeared white, indicative of numerous discontinuous polycrystals, but gradually became transparent as the temperature increased, even below 300 K. This transparency may arise from the formation of a surface layer filling the gaps between crystallites, with this layer corresponding to the surrounding region. Although only circumstantial, this observation may point toward the possibility of event (2). Additional experiments, particularly those aimed at elucidating the structure of the surface phase, are required to conclusively address this issue.

The second topic to discuss is whether the two distinct regions that appear above 300 K can be considered phases. The core region can naturally be considered a crystalline phase with a PC structure across the entire PC region. Conversely, the surrounding region below 300 K should not be considered a phase. The surrounding region arises from differences in environment between the core and the PC surface or grain boundaries filling the inter-crystallite spaces. Furthermore, from the perspective of T_2 values, it is impossible to distinguish the surrounding from the core region. However, as shown in Fig. 3 and 4, above 300 K, the surrounding region exhibits a consistent, fixed value and exists as a region with uniform physical properties. Therefore, above 300 K, we also consider the surrounding region to be a phase in terms of T_2 values.

The third point to consider is whether the emergence of two distinct regions at around 300 K is indicative of phase transitions. For the surrounding region, the T_2^{1C} value jumps to a T_2^{soft} value that is in several times larger. This clearly indicates the presence of a phase transition. Furthermore, actual experiments show the state around 300 K is unstable, making it difficult to reliably determine the T_2^{soft} values, which confirms our conviction that some phase transition exists. Conversely, T_2^{1C} connects smoothly with the T_2^{hard} value, leading us to initially conclude that no phase transition occurs in the core region. Regarding structural changes of PC crystal in this region, H. Abe (National Defense Academy) is currently conducting detailed experiments using X-ray diffraction and is expected to publish the results in the near future. According to his private correspondence, a phase transition is also occurring in the core region. In this region, neither the temperature dependence of NMR-T_1 nor the DSC chart shows any changes that are indicative of a phase transition. Therefore, this change, appearing solely in NMR-T_2, is concluded to be a higher-order phase transition with no enthalpy change, or at most a first-order phase transition with a very slight change. It is thought that the transition is induced by translational motion rather than molecular rotation.

3.7. Comparison of the heterogeneous dynamics in two types of plastic crystals

SN is a molecular compound that exhibits a PC phase. Detailed NMR relaxation time measurements have previously been performed for the PC phase of [C_2epyr][FSA], an ionic compound.[38,39] The present work enables a comparison between the relaxation time results of SN and those of [C_2epyr][FSA]. A comparison of the T_1 values for the two samples is not particularly meaningful, as T_1 primarily reflects the rotational and conformational transformations of the constituent molecules or molecular ions. Instead, the focus here is on comparing the T_2 behavior

of the two systems—that is, the translational dynamics of the molecules or molecular ions in the PC phase.

The magnitudes of the T_2 values for the two samples were compared. Because $1/T_2$ is positively correlated with the correlation time, τ_c, a larger T_2 value indicates more active motion. In the regular ordered crystal phases, both samples exhibited T_2 values on the order of 10^1 μs, with those for SN being slightly larger than those for [C_2epyr][FSA]. In the liquid phase, at temperatures slightly above the respective melting points, the T_2 values were on the order of 10^0 s, again slightly larger for SN. These observations suggest that the translational motions in SN are likely more active than those in [C_2epyr][FSA] in both the regular ordered crystal and liquid phases. This outcome is consistent with expectations based on the particle sizes and the interparticle interactions.

The T_2 behaviors of the two samples in the PC phase were then compared. The heterogeneous dynamics observed in [C_2epyr][FSA] were also present in SN, with the respective T_2 values separating into two components, namely T_2^{hard} and T_2^{soft}. However, in terms of magnitude, the trend in the PC phase was completely opposite to those observed in the ordered crystalline and liquid phases. In both the hard and soft phases, the T_2 values of SN were approximately two orders of magnitude lower than the corresponding ^{1}H-T_2 (or ^{19}F-T_2) values of [C_2epyr][FSA]. In other words, in the PC phase, SN molecules were less mobile than the $[C_2epyr]^+$ cations and $[FSA]^-$ anions.

In the case of SN (Fig. 3), the T_2^{core} curve obtained from the one-component analysis was smoothly connected to the T_2^{hard} curve at the separation point. At the melting point, both the T_2^{hard} and T_2^{soft} curves exhibited jumps to the T_2^{liq} (liquid-state T_2) curve. The behavior was different for [C_2epyr][FSA].[38,39] Notably, in [C_2epyr][FSA], the cation and anion dynamics could be observed separately, with the former reflected in the ^{1}H-T_2 data and the latter in the ^{19}F-T_2 data. At the separation point, the ^{1}H-T_2^{core} curve did not connect continuously to either the ^{1}H-T_2^{hard} or ^{1}H-T_2^{soft} curves. At the melting point, the ^{1}H-T_2^{hard} curve showed a jump to the ^{1}H-T_2^{liq} curve, whereas the ^{1}H-T_2^{soft} curve connected almost smoothly to the ^{1}H-T_2^{liq} curve. The ^{19}F-T_2 curves displayed analogous changes to the ^{1}H-T_2 curves. From the perspective of T_2 behaviour, in SN, the phase transition clearly occurs in the surrounding phase (T_2^{soft}), but cannot be detected by T_2 measurements in the core phase. (See Section 3.6). By contrast, in [C_2epyr][FSA], the phase transition at the separation point occurred in both the surrounding (T_2^{soft}) and core (T_2^{hard}) phases.

In the vicinity of the melting point, the translational behavior of the molecules in the core and surface phases of SN was qualitatively different from that in the liquid phase. By contrast, in [C_2epyr][FSA], the surface phase hardly underwent a phase transition—if any change occurred, it was negligible—and transitioned directly to the liquid state. These results indicate that, in terms of translational motion, the PC phase of SN exhibited more crystalline characteristics, whereas that of [C_2epyr][FSA] displayed more liquid-like characteristics. Although SN is a molecular compound and [C_2epyr][FSA] is ionic, this observation appears to contradict the general expectation. However, in [C_2epyr][FSA], both the cation and anion are bulky, reducing the strength of Coulomb interactions. Instead, the difference likely arises from the nature of the rotational motion: SN undergoes uniaxial molecular rotation, whereas in [C_2epyr][FSA], both ions rotate freely.

4. Conclusions

Heterogeneous dynamics in the PC phase have been reported for several IPCs in recent years. The primary objective of this study was to determine whether a similar phenomenon also occurs in MPCs.

SN was selected as a representative MPC, and the temperature dependences of the spin–lattice relaxation time (T_1) and spin–spin relaxation time (T_2) for ^{1}H were measured. The T_2 values, which are sensitive to translational motion, were found to split into two components in the PC phase region. These components corresponded to the existence of distinct regions: one in which SN molecules exhibited relatively active translational motion (soft component) and another in which they were less mobile (hard component). We believe that the heterogeneous translational dynamics of SN, like IPC, is attributable to the presence of two distinct static regions: the core region, which forms the PC phase and the surrounding region, which comprises the surface layer and grain boundaries.

As in IPCs, evidence of heterogeneous dynamics in SN appeared only in the T_2 values; no anomalies were observed in the T_1 values or in the DSC traces. The results lead to the conclusion that the heterogeneous dynamics in SN are induced by a higher-order phase transition or at most a first-order phase transition with a very slight change and that such dynamics appear to be an intrinsic property of plastic crystals, irrespective of whether they are ionic or molecular in nature.

The concept of heterogeneous dynamics was initially discussed in research concerning the glass transition in some PCs.[54] In contrast, the present phenomenon relates to the partial softening of the PC phase. In other words, we consider the former to be a phenomenon associated with glass formation, and the latter with melting *via* surface melting.

Author contributions

All authors were involved in the conception of the project and the discussion on the methodology and experimental results. K. N.: NMR experiments and their analysis, interpretation of NMR results, and manuscript writing. K. F.: NMR experiments and their analysis and interpretation of NMR results.

Conflicts of interest

There are no conflicts to declare.

Data availability

The data supporting this article have been included in the supplementary information (SI). Supplementary information is available. See DOI: https://doi.org/10.1039/d5cp03114a.

Acknowledgements

We would like to thank Professor Kazuhiko Matsumoto (Kyoto University), Professor Masahiro Yoshizawa-Fujita (Sophia University) and Professor Hiroshi Abe (National Defense Academy of Japan) for helpful discussion. This study was partly supported by JSPS KAKENHI (Grant Number 19H02671 for K.N.).

References

1 J. Timmermans, *J. Phys. Chem. Solids*, 1961, **18**, 1–8.
2 I. Nitta, *Z. Kristallogr. - Cryst. Mater.*, 1959, **112**, 234–254.
3 W. J. Dunning, *Phys. Chem. Solids*, 1961, **18**, 21–27.
4 S. Seki, *Chem. Chem. Ind.*, 1962, **15**, 1226–1236.
5 L. A. K. Sravery, *Ann. Rev. Phys. Chem.*, 1962, **13**, 351–368.
6 ed. J. N. Sherwood, *The plastically crystalline state—orientationally disordered crystals*, John Wiley & Sons, Chichester, 1979.
7 D. R. MacFarlane, J. Huang and M. Forsyth, *Nature*, 1999, **402**, 792–794.
8 D. R. MacFarlane, P. Meakin, J. Sun, N. Amini and M. Forsyth, *J. Phys. Chem. B*, 1999, **103**, 4164–4170.
9 D. R. MacFarlane and M. Forsyth, *Adv. Mater.*, 2001, **13**, 957–965.
10 J. M. Pringle, P. C. Howlett, D. R. MacFarlane and M. Forsyth, *J. Mater. Chem.*, 2010, **20**, 2056–2062.
11 R. Yunis, D. Al-Masri, A. F. Hollenkamp, C. M. Doherty, H. Zhu and M. Pringle, *J. Electrochem. Soc.*, 2020, **167**, 070529.
12 J. M. Pringle, *Phys. Chem. Chem. Phys.*, 2013, **15**, 1339–1351.
13 H. Zhu, D. R. MacFarlane, J. M. Pringle and M. Forsyth, *Trends Chem.*, 2019, **1**, 126–140.
14 J. Hwang, K. Matsumoto, C. Y. Chen and R. Hagiwara, *Energy Environ. Sci.*, 2021, **14**, 5834–5863.
15 K. Hayamizu, S. Tsuzuki and S. Seki, *J. Phys. Chem. A*, 2008, **112**, 12027–12036.
16 K. Hayamizu, S. Tsuzuki, S. Seki and Y. Umebayashi, *J. Phys. Chem. B*, 2012, **116**, 11284–11291.
17 H. Zhu and L. A. O'Dell, *Chem. Commun.*, 2021, **57**, 5609–5625.
18 H. Ishida, T. Iwachido and R. Ikeda, *Ber. Bunsenges. Phys. Chem.*, 1992, **96**, 1468–1470.
19 H. Ishida, T. Takagi and R. Ikeda, *Chem. Lett.*, 1992, 605–608.
20 H. Ono, R. Seki, R. Ikeda and H. Ishida, *J. Mol. Struct.*, 1995, **345**, 235–243.
21 H. Ishida, Y. Furukawa, S. Kashino, S. Sato and R. Ikeda, *Ber. Bunsenges Phys. Chem.*, 1996, **100**, 433–439.
22 J. Adebahr, A. J. Seeber, D. R. MacFarlane and M. Forsyth, *J. Phys. Chem. B*, 2005, **109**, 20087–20092.
23 L. Jin, K. M. Mairn, C. M. Forsyth, A. J. Seeber, D. R. MacFarlane, P. C. Howlett, M. Forsyth and J. M. Pringle, *J. Am. Chem. Soc.*, 2012, **134**, 9688–9697.
24 I. Jin, S. Leeuw, M. V. Koudriachova, J. M. Pringle, P. C. Howlett, F. Chen and M. Forsyth, *Phys. Chem. Chem. Phys.*, 2013, **15**, 19570–19674.
25 L. Jin, K. M. Nairn, C. D. Ling, H. Zhu, L. A. O'Dell, J. Li, F. Chen, A. F. Pavan, L. A. Madsen, P. C. Howlett, D. R. MacFarlane, M. Forsyth and J. M. Pringle, *J. Phys. Chem. B*, 2017, **121**, 5439–5446.
26 M. Forsyth, F. Chen, L. A. O'Dell and K. Romanenko, *Solid State Ionics*, 2016, **288**, 160–166.
27 K. Romanenko, L. Jin, L. A. Madsen, J. M. Pringle, L. A. O'Dell and M. Forsyth, *J. Am. Chem. Soc.*, 2014, **136**, 15638–15645.
28 K. Romanenko, J. M. Pringle, L. A. O'Dell and M. Forsyth, *Phys. Chem. Chem. Phys.*, 2015, **17**, 18991–19000.
29 M. Imanari, K. Uchida, K. Miyano, H. Seki and K. Nishikawa, *Phys. Chem. Chem. Phys.*, 2010, **12**, 2959–2967.
30 T. Endo, T. Imanari, H. Seki and K. Nishikawa, *J. Phys. Chem. A*, 2011, **115**, 2999–3005.
31 T. Endo, H. Murata, M. Imanari, N. Mizushima, H. Seki and K. Nishikawa, *J. Phys. Chem. B*, 2012, **116**, 3780–3788.
32 M. Imanari, K. Fujii, T. Endo, H. Seki, K. Tozaki and K. Nishikawa, *J. Phys. Chem. B*, 2012, **116**, 3991–3997.
33 T. Endo, S. Widgeon, P. Yu, S. Sen and K. Nishikawa, *Phys. Rev. B:Condens. Matter Mater. Phys.*, 2012, **85**, 054307.
34 T. Endo, H. Murata, M. Imanari, N. Mizushima, H. Seki, S. Sen and K. Nishikawa, *J. Phys. Chem. B*, 2013, **117**, 326–332.
35 M. Imanari, K. Fujii, T. Mukai, N. Mizushima, H. Seki and K. Nishikawa, *Phys. Chem. Chem. Phys.*, 2015, **17**, 8750–8757.
36 Y. Shimizu, Y. Wachi, K. Fujii, M. Imanari and K. Nishikawa, *J. Phys. Chem. B*, 2016, **120**, 5710–5719.
37 K. Nishikawa and K. Fujii, *Bull. Chem. Soc. Jpn.*, 2023, **96**, 931–937.
38 K. Nishikawa, K. Fujii, K. Matsumoto, H. Abe and M. Yoshizawa-Fujita, *Bull. Chem. Soc. Jpn.*, 2024, **97**, uoae088.
39 K. Nishikawa, K. Fujii and M. Yoshizawa-Fujita, *Phys. Chem. Chem. Phys.*, 2025, **27**, 15126–15136.
40 P.-J. Alarco, Y. Abu-Lebdeh, A. Abouimrane and M. Armand, *Nat. Mater.*, 2004, **3**, 476–481.
41 T. C. Farrar and E. D. Becker, *Pulse and Fourier Transform NMR, Introduction to Theory and Method*, Academic Press, New York, 1971.
42 E. Badea, I. Blanco and G. D. Gatta, *J. Chem. Thermodyn.*, 2007, **39**, 1392–1398.
43 S. Hore, R. Dinnebier, W. Wen, J. Hanson and J. Maier, *Z. Anorg. Allg. Chem.*, 2009, **635**, 88–93.
44 P. Derollez, J. Lefevre, M. Descamps, W. Press and H. Fontaine, *J. Phys.: Condens. Matter*, 1990, **2**, 6893–6903.
45 K. Nishikawa, T. Yamada, K. Fujii, H. Masu, K. Tozaki and T. Endo, *Bull. Chem. Soc. Jpn.*, 2021, **94**, 2003–2010.
46 K. Nishikawa, K. Fujii, T. Yamada, M. Yoshizawa-Fujita and K. Matsumoto, *Chem. Phys. Lett.*, 2022, **803**, 139771.
47 M. Canales, I. Skarmoutsos and E. Guardia, *J. Chem. Phys.*, 2024, **161**, 174503.
48 T. Fijiyama, K. Tokumaru and T. Schimanouchi, *Spectrochim. Acta*, 1964, **20**, 415–428.
49 J. Nowak, J. Małecki, J. Thiébaut and J. Rivail, *J. Chem. Soc., Faraday Trans. 2*, 1980, **76**, 197–204.
50 T. Bauer, M. Köhler, P. Lunkenheimer, A. Loidl and C. A. Angell, *J. Chem. Phys.*, 2010, **133**, 144509.

51 M. Götz, Th Bauer, P. Lunkenheimer and A. Loidl, *J. Chem. Phys.*, 2014, **140**, 094504.
52 J. L. Tamarit, I. B. Rietveld, M. Barrio and R. Céolin, *J. Mol. Struct.*, 2014, **1078**, 3–9.
53 V. S. Kandagal, F. Chen, J. M. Plingle and M. Forsyth, *J. Phys. Chem. B*, 2018, **122**, 8274–8283.
54 R. Brand, P. Lunkenheimer and A. Loidl, *J. Chem. Phys.*, 2002, **116**, 10386.